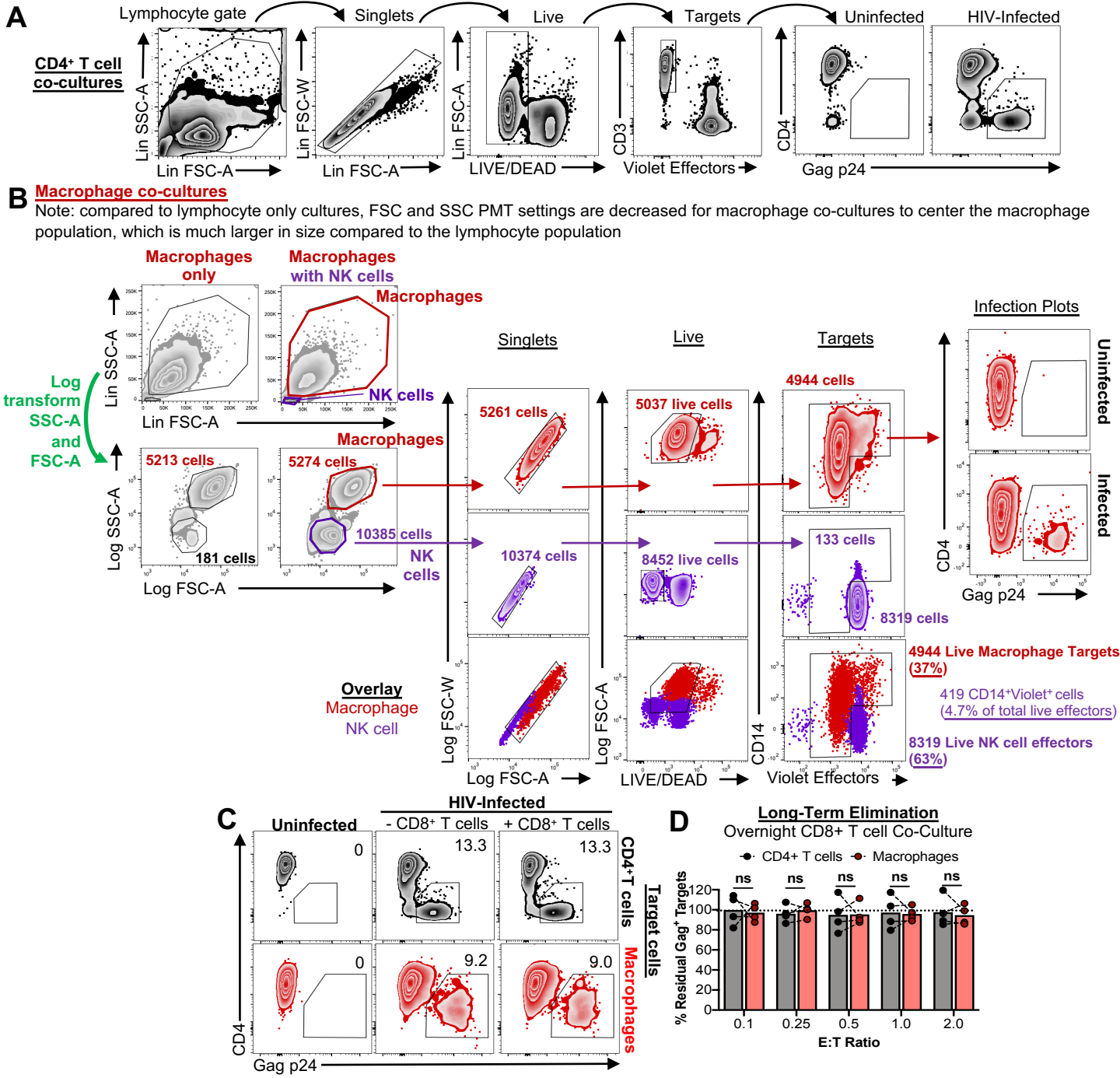

Fig. S1. Elimination assay gating and control elimination assays related to Fig. 1. (A) Gating strategy for the HIV-infected CD4⁺ T cell targets subjected to an elimination assay. NK cells were stained with CellTrace Violet to distinguish target cells from effector cells. Shown are plots from a 4-hour elimination assay. **(B)** Gating strategy for the HIV-infected macrophage targets subjected to an elimination assay. Note, forward scatter (FSC) and side scatter (SSC) PMT settings were lowered to center on the macrophage population, which was significantly larger than the effectors. Thus, the macrophage targets (red gate) were initially excluded from the effector cells (purple gate) based on size. This allows for a cleaner separation of the target and effector cells as including the effectors in the initial gating ("Overlay") makes distinguishing live macrophages from dead NK cells difficult (middle plot of overlay). Of the live macrophages, CD14⁺Violet⁺ cells represent macrophages that have phagocytosed a small portion of effectors, which were included in the analysis of infected target cells. The majority of the live effectors (CD14⁻Violet⁺) are not phagocytosed. Shown are plots from a 4-hour elimination assay. Similar results were observed with an overnight elimination assay. **(C and D)** Target cell elimination by bulk autologous *ex* vivo CD8⁺ T cells from healthy donors. **(C)** Shown are representative elimination assay plots. **(D)** Summary data for elimination assays performed overnight at multiple E:T ratios. Data are from two independent experiments (n=4 biological replicates). Statistical analysis: paired t test, ns = not significant.

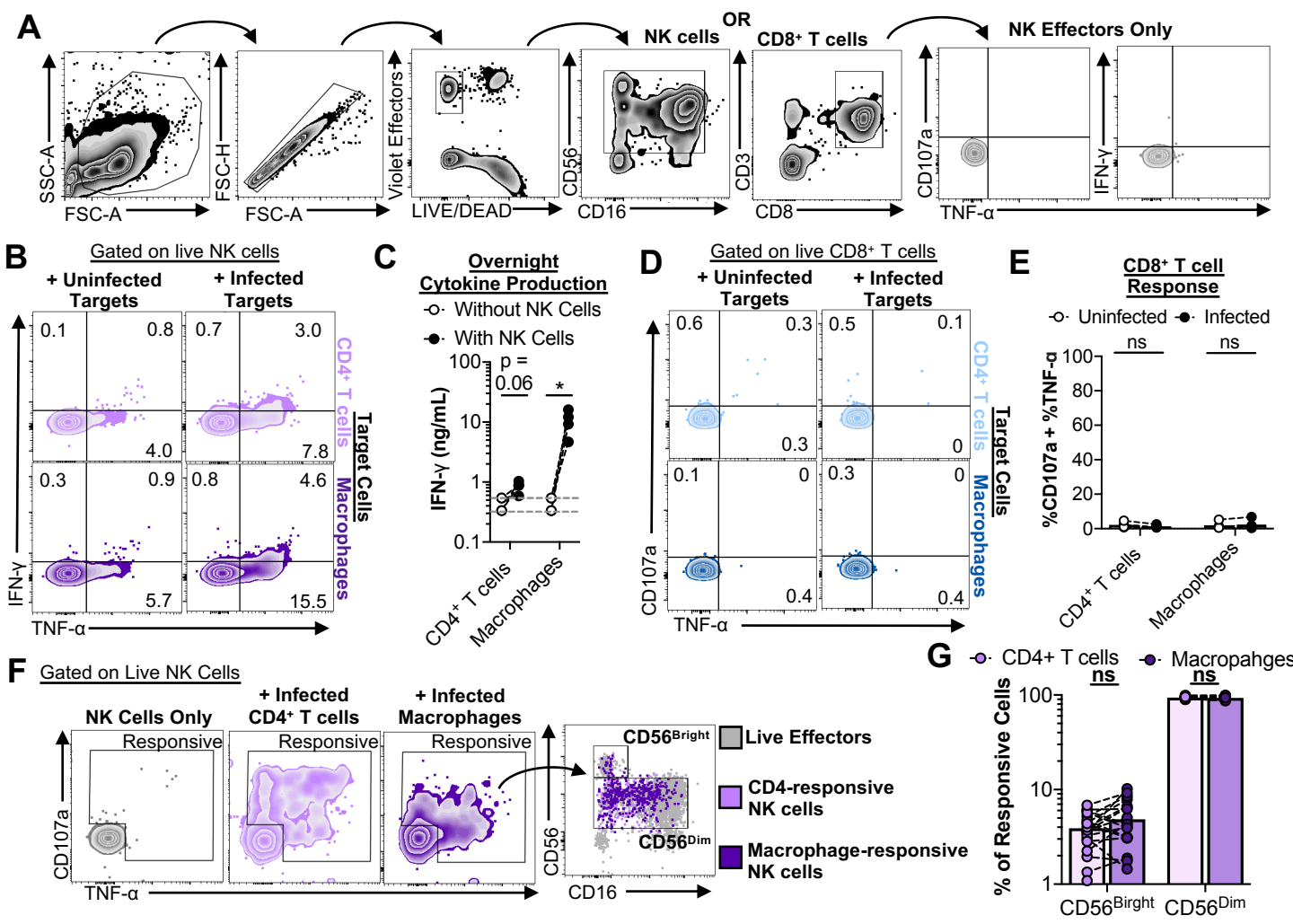

Fig. S2. Recognition assay gating and control recognition assays related to Fig. 2. (A) Gating strategy for the NK cell-target co-culture recognition assays. NK cell or CD8⁺ T cell effectors were stained with CellTrace Violet to distinguish target cells from effectors cells. Additional stains for CD56/CD16 or CD3/CD8 were used to gate on true NK cells or CD8⁺ T cells. Cultures with only effector cells were used to establish gating for degranulation/CD107a and TNF-α/IFN-γ responses (grey plots). Shown are representative TNF-α/IFN-γ plots from NK cell cultures; similar plots were observed with CD8⁺ T cell-only cultures. **(B)** TNF-α, not IFN-γ, is the predominant NK cell cytokine produced in short-term NK cell-target co-cultures as measured by intracellular cytokine staining following a 6-hour co-culture recognition assay. Shown are representative flow cytometry plots from 14 independent experiments. **(C)** IFN-γ, as measured by ELISA, is observed after overnight NK cell co-cultures, but not in cultures of infected CD4⁺ T cells and macrophages in the absence of NK cell effectors, or in NK only cultures. Gray dotted lines indicate the range of the limits of detections for each of the individual experiments. Readings for NK cell-only cultures were below the limits of detection. Shown are data from two independent experiments (n=4 biological replicates). Statistical analysis, paired t test: *p<0.05. **(D and E)** Recognition of infected targets by bulk autologous *ex vivo* CD8⁺ T cells from healthy donors after 6 hours at a target-to-effector (T:E) ratio of 10. **(D)** Shown are representative CD8⁺ T cell recognition assay plots. **(E)** Summary data from three independent experiments (n=4 biological replicates). Statistical analysis: paired t test, ns=not significant. **(F and G)** CD56 phenotype of NK cells responding to infected CD4⁺ T cells and macrophages. "Responsive" gates were drawn to include all CD107a⁺ and TNF-α⁺ cells. The CD56 phenotype (Bright or Dim) of the cells was then determined based on CD56/CD16 plots. **(F)** Shown are representative plots of the "Responsive", $CD56^{Bright}$, and $CD56^{Dim}$ gates. **(G)** Shown are results from ten independent experiments (n=16 biological replicates). Statistical analysis: paired t test, ns=not significant.

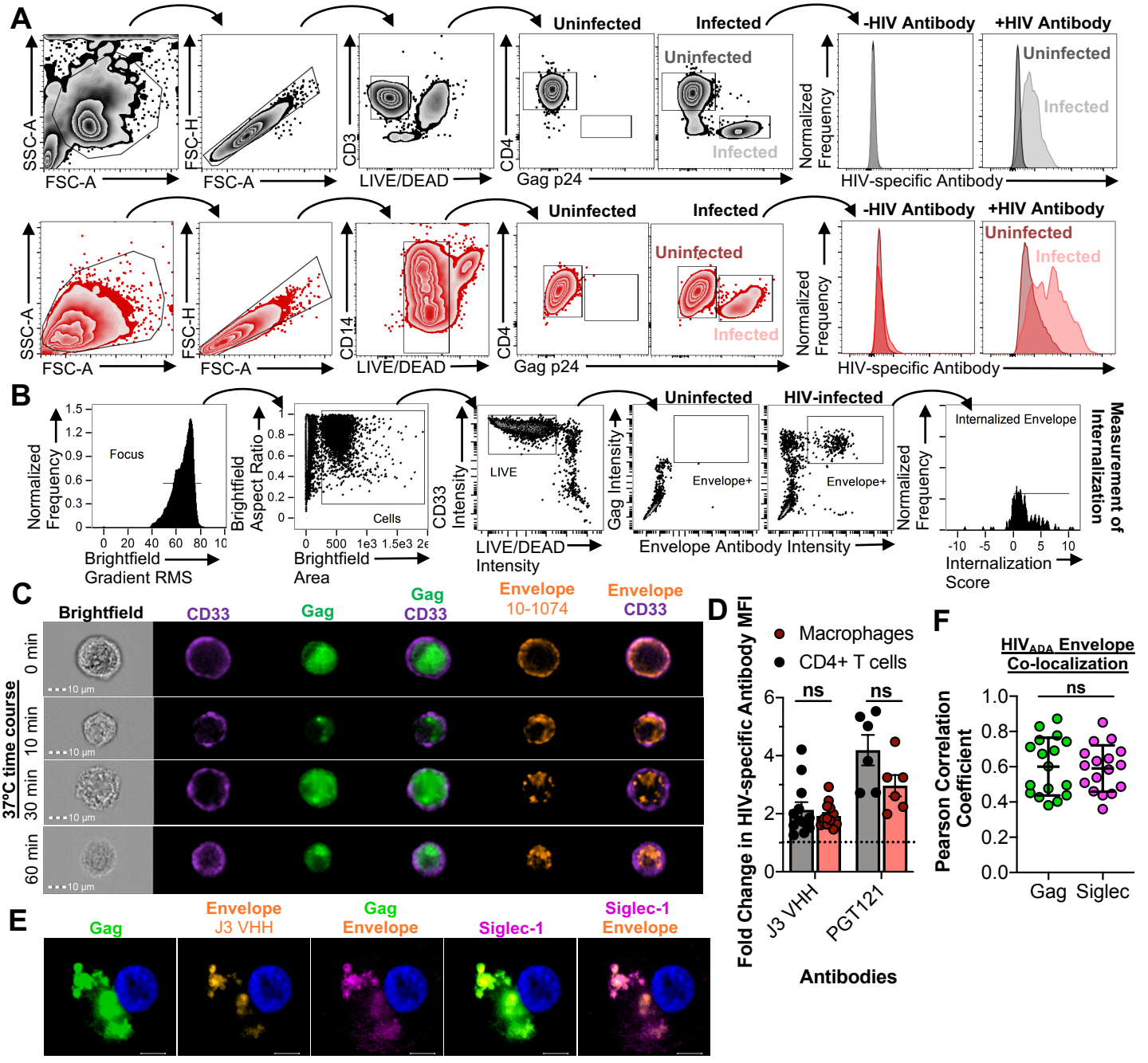

Fig. S3. Detection of the surface HIV envelope using HIV envelope-specific antibodies related to Fig. 3. (A) Gating strategy for the envelope staining on HIV-infected CD4⁺ T cells (black plots) and macrophages (red plots). **(B and C)** ImageStream analysis of the HIV envelope internalization on infected macrophages. Description of the experimental setup can be found in Fig. 3 and the STAR Methods. **(B)** ImageStream gating strategy. Internalization scores and graphs for the HIV Gag and Envelope antibodies were generated by the IDEAS Software Internalization Wizard using CD33 as the surface probe. **(C)** Representative images of the HIV envelope antibody 10-1074 internalization over 60 minutes. **(D-F)** Characterization of the HIV envelope on HIV_{ADA}-infected cells. **(D)** Summary of the "Fold change in HIV-specific Antibody MFI" for J3 VHH and PGT121. Explanation of the calculations can be found in the STAR Methods. Data were collected across a total of 11 independent experiments. Statistical analysis, unpaired t test, ns=not significant. **(E)** Characterization of the internalized HIV envelope on HIV_{ADA}-infected macrophages using confocal microscopy. Description of the experimental setup can be found in the STAR Methods. Shown are representative images of infected macrophages stained for the HIV Gag, Envelope (J3 VHH), and Siglec-1. Blue staining is Hoescht/Nuclei. The bar denotes 10µm. **(F)** Summary of the HIV envelope co-colocalization with the HIV Gag and Siglec-1. Shown are the calculated Pearson Correlation Coefficients for Envelope vs Gag and Envelope vs Siglec-1 (n=17 images over 2 independent experiments). Statistical analysis: unpaired t test, ns=not significant.

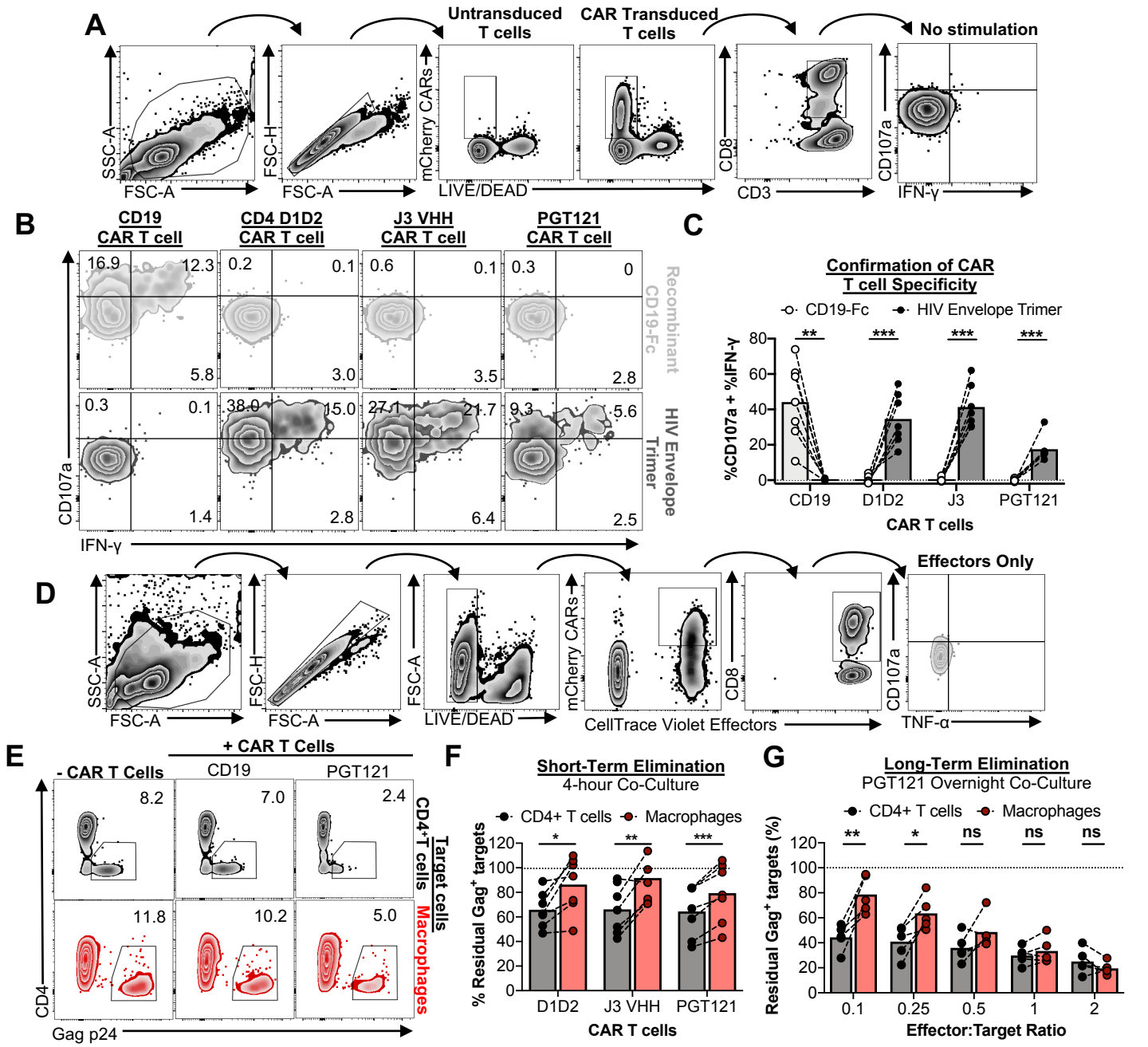

Fig. S4. CAR T cell characterization related to Fig. 4. (A-C) CAR T cell validation. ~14 days post-transduction, the cells were plated onto recombinant CD19-Fc or recombinant HIV envelope gp140-coated plates, incubated for 6 hours and then assessed for CD107a and IFN-γ production via flow cytometry. **(A)** Gating strategy for the CAR T cell recognition assays. mCherry was used to distinguish CAR T cells. CAR T cells stimulated on buffer-coated plates were used to establish the gating for CD107a and IFN-γ production. **(B)** Shown are representative recognition assay plots. **(C)** Summary data from four independent experiments (n=7 biological replicates). %CD107a+%IFN-γ values are corrected for background recognition of cells stimulated with no antigen. Statistical analysis: paired t test, **p<0.01, ***p<0.001. **(D)** Gating strategy for the CAR T cell recognition assays with HIV-infected targets. CAR T cell effectors were stained with CellTrace Violet to distinguish target cells from effectors cells. Cultures with only effector cells were used to establish the gating for CD107a and TNF-α. **(E-G)** HIV-infected target cell elimination by CAR T cells. Gating strategy for the elimination assays are shown in Fig. S1. **(E)** Shown are representative elimination assay plots. **(F)** Summary data from four independent experiments (n=7 biological replicates) for 4-hour elimination assays at an E:T ratio of 4. Values are corrected for background elimination seen with CD19-specific CAR T cells Statistical analysis: paired t test, *p<0.05, **p<0.01, ***p<0.01. **(I)** Summary data from three independent experiments (n=5 biological replicates) for overnight elimination assays. Values are corrected for background elimination seen with CD19-specific CAR T cells. Statistical analysis: paired t test, *p<0.05, **p<0.01, ns=not significant.

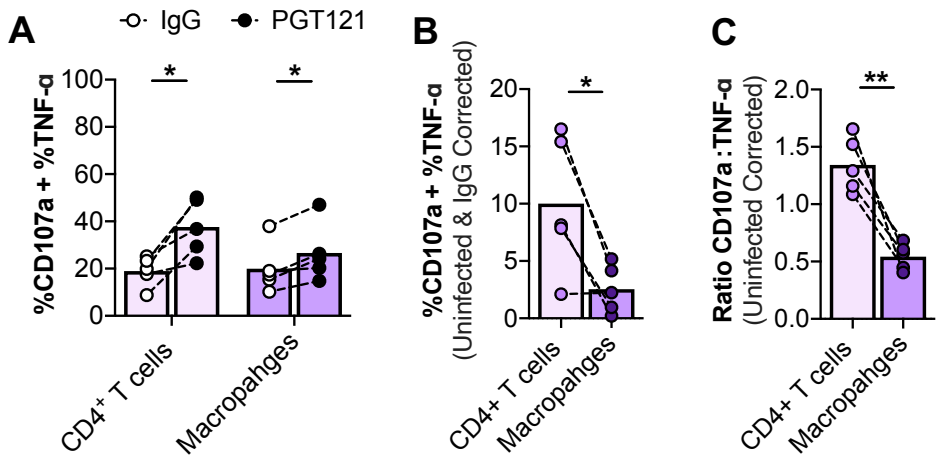

Fig. S5. NK ADCC recognition assays for HIV_{ADA}-infected targets related to Fig 5. NK cell HIV envelope-specific ADCC-mediated recognition of HIV_{ADA}-infected targets. NK cells were incubated with targets at a T:E of 10 +/- normal human IgG (negative control) or PGT121 at 30ug/mL for 6 hours, followed by flow cytometry analysis of degranulation/CD107a and TNF-α production. The gating strategy for live NK cells is shown in Fig. S2. Shown are results from three independent experiments (n=5 biological replicates). Statistical analysis: paired t test, *p<0.05, **p<0.01. **(A)** HIV-specific ADCC enhances responses to both infected $CD4^+$ T cells and macrophages. Data summaries for NK cell responses (%CD107a + %TNF-α). **(B)** Total NK cell ADCC responses to infected macrophages are significantly lower compared to ADCC responses to $CD4^+$ T cells. "%CD107a + %TNF-α" values are initially corrected for background responses to uninfected targets and normalized to target cell infection frequencies, followed by correction for responses in IgG conditions. **(C)** Data summaries for the quality of the NK cell response. Values are corrected for background responses to uninfected target cells. Ratios of degranulation/CD107a versus TNF-α production were calculated as described in the STAR Methods.

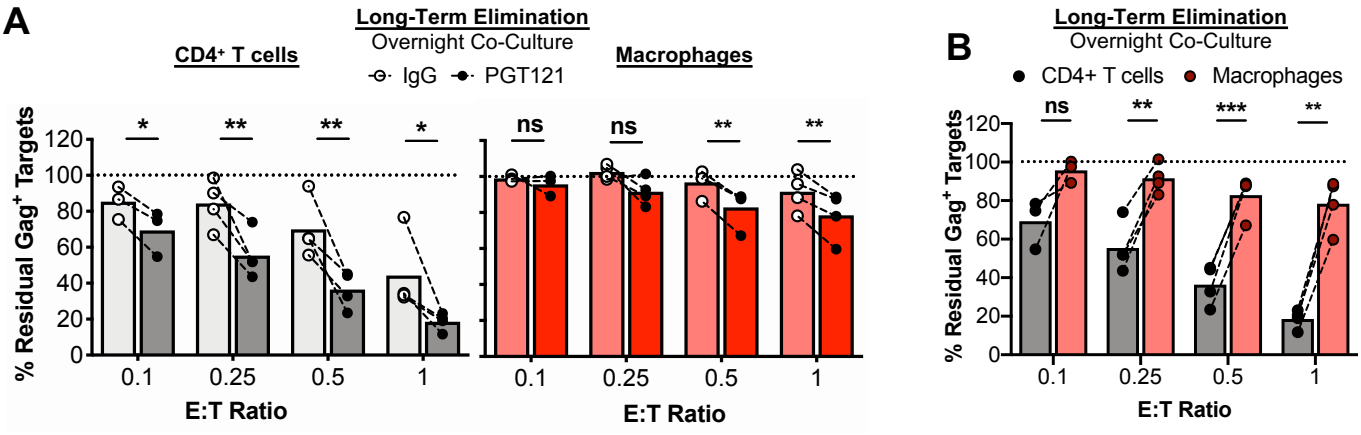

Fig. S6. NK ADCC elimination assays for HIV_{ADA}-infected targets related to Fig. 6. NK cell elimination of HIV_{ADA}-infected targets. HIV-infected $CD4^+$ T cells and macrophages were co-cultured overnight +/- autologous NK cells with either human IgG or PGT121 at multiple E:T ratios followed by flow cytometry-based analysis of residual target cell infection by intracellular Gag p24 staining. Gating strategy is shown in Fig. S1. **(A)** PGT121-specific ADCC elimination of infected targets and **(B)** the differences in ADCC elimination of infected $CD4^+$ T cells and macrophages. Shown are results from three independent experiments (n=5 biological replicates). Statistical analysis: paired t test, *p<0.05, **p<0.01, ***p<0.001, ns=not significant.